# OPTIMIZATION OF A NANOSTRUCTURED LIPID CARRIERS SYSTEM FOR ENHANCING THE BIOPHARMACEUTICAL PROPERTIES OF VALSARTAN

M. A. ALBEKERY[a], K. T. ALHARBI[a], S. ALARIFI[a,b], D. AHMAD[a,b], M. E OMER[a,b], S. MASSADEH[b], A. E. YASSIN[a,b*]
[a]*College of Pharmacy, King Saud bin Abdulaziz University for Health Sciences,*
[b]*King Abdullah International Medical Research Center, and King Abdulaziz Medical City, Ministry of National Guard, Health Affairs, Riyadh, Saudi Arabia*

To optimize a nanostructured lipid carriers system (NLC) for the per-oral delivery of valsartan (Val), a model BCS class II drug, in an attempt to enhance its therapeutic performance by increasing both solubility and dissolution. Val-loaded NLCs were prepared using ultrasonic melt-emulsification method. Number of formulation factors including the type of oil/lipid, Val to lipid ratio, and surfactant ratio were investigated. The prepared NLC were evaluated for their particle size and shape, polydispersity index, zeta potential, and drug entrapment efficiency. The *in vitro* drug release profiles were evaluated using a dialysis bags with cut-off 12KD. The prepared NLCs showed average sizes between 423.99±12.73 and 805.53±39.5 nm, and polydispersity index in the range of 0.287 to 0.361. The zeta-potential values were between -3.34 and -10.59 mV. The entrapment efficiency was not very high between 27.3 to 75.04%. The scanning electron images showed almost spherical shapes with sizes lower than those obtained by light scattering. The *in vitro* release followed a bi-phasic pattern with an initial rapid Val release followed by a slow release varying according to the composition. Two formulations F2 and F4 showed complete drug release within the first two hours. The optimum surfactant ratio was 37.5% by weight of the total lipid. NLC successfully enhanced the Val release rate and dissolution with high potential to enhance its bioavailability.

(Received January 16, 2017; Accepted May 8, 2017)

*Keywords:* ultrasonic melt-emulsification, stearic acid, Dynasan, zeta-potential

## 1. Introduction

The field of nano-drug delivery is widely spreading in the last decade with more medical applications for both diagnosis and treatment of many diseases (1). They tend to exploit a number of beneficial attributes of nanomaterials including the high surface energy which allow them to interact with biomolecules on the cell surface of cells and the ability to form a homogenous dispersion in biological media. Various drug delivery systems were assembled basically from lipid material. These include liposomes, nanoemulsion, microemulsion, lipoplexes, solid lipid nanoparticles (SLN), and Nano structured lipid carriers (NLC). Liposomes were extensively employed in improving the efficacy of many drugs such as doxorubicin (2), methotrexate (3), and amphotericin B (4). Lipoplexes are lipid based complexes assembled from an oppositely charged lipid and a drug. They were successfully utilized in the delivery of siRNA (5) and pDNA (6).

Self-nanoemulsifying drug delivery systems (SNEDDS) are designed by mixing oils, surfactant and co-surfactant in an optimum ratio that allow prompt formation of O/W emulsion with nano globule size when mixed with the gastric medium (7).

SLN are relatively new pharmaceutical delivery systems made of sub-micron (between 10 and 1000 nm) colloidal lipid drug carriers with relatively above ambient melting points which remain solid at room temperature as well as body temperature (8). They showed a number of attractive properties that make them successful alternative to conventional nano-carriers such as liposomes, polymeric nanoparticles and nano-emulsions (9). The main advantages of SLN include

*Corresponding author: yassina@ksau-hs.edu.sa.

high drug loading capacity, high biocompatibility, more resistant to chemical degradation, and enhanced stability of liable pharmaceuticals (1, 10-14). The possibility of production with industrial techniques such as high pressure homogenization made them highly attractive to the pharmaceutical industry as the cost of production is much lower (14, 15) . SLN can be administered through a variety of routes including; oral, parenteral, nasal, pulmonary, transdermal, and ocular (12,13, 16-18).

On the other hand, SLN possess some limitations including; possibility of particle growth, high burst release, and compromised stability in tropical climates (14,19, 20). NLC were introduced to avoid such limitations (21). Incorporation of oil that solubilizes the drug and using a combination of lipids with different hydrocarbon chain length are the main approaches employed in the design of NLC system (22, 23). NLC were successfully used to enhance the solubility and/or intestinal permeability of many Biopharmaceutical Classification System (BCS) class II drugs such as clotrimazole and itraconazole and class IV drugs such as saquinavir (8, 24, 25).

SLN and NLC can be prepared by numerous methods such as high speed homogenization, high pressure homogenization, double emulsion, solvent emulsification and evaporation, super critical fluid, and spray-drying (11-14, 17, 20, 26, 27). All the methods depend on the emulsification of melted lipids or solutions of lipids in organic solvents with aqueous surfactant solutions and adjusting the globule sizes to the nanoscale (28).

Valsartan (Val), the angiotensin II receptor blocker antihypertensive drug, is suggested as a BCS class II model drug. It suffers a low bioavailability (only 23%) as a result of its poor aqueous solubility (29). This study aims to optimize a NLC system for the per-oral delivery of a model BCS class II drug, valsartan, in an attempt to enhance its therapeutic performance by increasing both solubility and dissolution.

## 2. Materials and methods

### 2.1. Materials

Val was obtained as a gift from Riyadh Pharma Medical & Cosmetic Products CO., Riyadh, Saudi Arabia. Dynasan™118, Softisan™ 154, and Imwitor were obtained from Sasol Germany GmbH (Witten, Germany). Stearic acid, Tween 80, castor oil, Neem oil and sodium deoxycholate were purchased from Sigma-Aldrich Chemical Co. (St Louis, MO, USA). All other reagents and chemicals were of analytical grade.

### 2.2. Methods

Preparation of Valsartan loaded NLC:

Simply, oily solution of Val was mixed with certain quantity of a melted lipid material at temperature 10°C above the lipid melting point. An aqueous surfactant solution was prepared by dissolving certain weights of Tween 80 and sodium deoxycholate. The surfactant solution was further heated to the same temperature degree and mixed with the oily lipid drug solution by probe-sonication for 3 min. to form an emulsion. Then, the formed emulsion was dispersed in cooled water by magnetic stirring for 10 min. The formed NLC were separated by centrifugation. Samples from the supernatant were taken and analyzed for the concentration of Val using a validated HPLC method. The residues were subjected to two cycles of re-dispersion in chilled water and centrifugation in order to wash away any un-entrapped Val. Afterward, samples were lyophilized using a freeze-dryer (Christ Beta 2-8 LD Plus, Martin Christ, Germany). Table 1 shows the exact composition of all the prepared formulas.

*Table 1: The composition and properties of each of the prepared valsartan nano-structured lipid carriers' formulations.*

| Formulation | Drug :Lipid ratio | Lipid used mg | | | | Surfactant | |
|---|---|---|---|---|---|---|---|
| | | stearic acid | Castor oil | Imwitor 900 | Dynasan 118 | Tween 80 | sodium deoxycholate |
| F1 | 1:9 | 337.5 | 112.5 | - | - | 25% | 12.5% |
| F2 | 1:9 | 337.5 | 112.5 | - | - | 33.3% | 16.7% |
| F3 | 1:9 | 337.5 | 112.5 | - | - | 15% | 7.5% |
| F4 | 1:9 | 168.8 | 112.5 | 168.8 | - | 25% | 12.5% |
| F5 | 1:9 | 253.1 | 112.5 | - | 84.4 | 25% | 12.5% |

Evaluation of the prepared solid lipid nanoparticles:

Measurement of particle size and zeta potential:

Photon correlation spectroscopy (PCS) were used to measure the mean particle size and polydispersity index of the size distribution. Samples of dried NLC were dispersed in distilled water by vortex mixing to give homogenous dispersion of ~ 0.1% w/v. The particle size was determined by photon correlation spectroscopy utilizing a Brookhaven ZetaPALS (Brookhaven Instruments Corporation, Holtsville, NY, USA). A 90° angle of detection was employed for all measurements.

Measurement of zeta potential:

Samples from the dispersions used in determination of particle size were evaluated for the determination of zeta potential by Laser Doppler Velocimetry (LDV) mode using the same Brookhaven at 25$^{o}$C. Each value reported is the average of five measurements.

Measurement of drug entrapment efficiency and drug loading:

The amounts of un-entrapped Val in the supernatant obtained after centrifugation of nanoparticles were determined using HPLC. The percentage drug entrapment efficiency (%EE) in each of the prepared formula was calculated according to the following formulas.

$$\% EE = \frac{\text{W initial drug} - \text{W free drug}}{\text{W initial drug}} X\ 100$$

The % drug loading (DL%) was estimated by dissolving a known weight of the lyophilized NPs in acetone and the concentrations were determined by HPLC according to the following formula

$$\% DL = \frac{\text{Amount of entrapped Val}}{(\text{Sample weight})} X\ 100$$

HPLC method:

A simple sensitive HPLC method was used for the determination of Val. The HPLC system consisted of Agilent 1200 series equipped with Photodiode Array Detector of 1260 series (Agilent, CA, USA). An Eclipsed XBD column (Agilent -PN 993967) C18, 150 mm x 3.0 mm i.d. with particle size of 5 µm was used for the separation and quantification. The mobile phase consisted of phosphate buffer (pH 3.6, 0.01 M): acetonitrile: methanol (46:44:10 v/v/v) and was filtered through a 0.45 µm filter and degassed before use. The injection volume was 20 µL. Analyses were run at a flow-rate of 1 mL min$^{-1}$ at an ambient temperature (25$^{0}$C) and detection

was conducted at λ = 265 nm. The peak areas were integrated automatically by using mass hunter® software. Under these conditions, VAL was eluted at 3.515 min.

The particle morphology:

The particle surface morphology of the Val loaded NLC was visualized by scanning electron microscopy (JSM-6360 LV, JEOL, Tokyo, Japan). The freeze-dried samples were fixed on carbon tape and sputter-coated with a thin gold layer under an argon atmosphere using a gold sputter module in a high-vacuum evaporator (JFC-1100 fine coat ion sputter; JEOL). Acceleration voltage of 10KV was employed for scanning and production of photomicrographs of the coated samples.

Differential scanning calorimetry (DSC)

The thermograms of pure Val, Val-free NLC, and some NLC formulations were developed utilizing a Netzsch DSC 214-Polyma differential scanning calorimeter (Bavaria, Germany) equipped with an intercooler. Indium/zinc standard were used for the calibration of the temperature and enthalpy scale. The samples were hermetically sealed in aluminum pans and heated over a temperature range of -25 – 150 °C under nitrogen gas purged at a flow rate of 50 ml/min. A constant flow rate of 10°C/min was employed.

In-vitro release profile study:

Certain weights from each formulation equivalent to 1 mg of Val were dispersed in 1ml of phosphate buffer and placed in a dialysis tube. The tube were tied from both ends and immersed in 20ml phosphate buffer pH 6.8 inside a stoppered flask. The flasks were incubated in a shaking water bath (SW22, Julabo, Allentown, PA, USA) at 37±1°C and 80 rpm shaking speed. At predetermined time intervals, samples of 1ml were withdrawn and replaced by fresh pre-heated medium to maintain sink condition. The % Val released were determined in each sample using HPLC.

## 3. Results and discussion

Mean particle size, zeta potential, percent entrapment efficiency, and percent drug loading measurements for all formulations are presented in Table 2. Fig. 1 shows comparison of the particle sizes for all the prepared NLC formulations. The prepared NLC formulations showed particle sizes in the range of 423.99 - 805.53 nm. It is clear that the particle size is dependent on lipid to surfactant ratio as F2 (containing a total of 50% surfactants from the total lipid and oil) showed the lowest particle size. The use of lipid combination also affected the particle size. F4 (containing 1:1 Stearic acid to Dynasan) had a significantly lower particle size 549.12±9.8 nm ($p < 0.05$) compared with 805.53±18.5 nm for F1 (containing stearic acid alone). Lower lipid combination ratios resulted in moderate reduction in particle size as seen with F5 (containing 3:1 stearic acid to Imwitor). It showed 700.12±21.23 nm. The polydispersity index is a useful parameter to indicate the degree the particle size uniformity. It was agreed upon in the literature that values of less than 0.3 are considered narrow size distribution ranges while values of less than 0.1 are indicated as single-disperse particles (30). From Table 2 and Fig. 2, it is clear that F2, F4, and F5 exhibited a narrow range of particle size distribution with polydispersity indices below 0.3 while both F1 and F3 had values higher than 0.3. F4 showed the lowest polydispersity index value of 0.287.

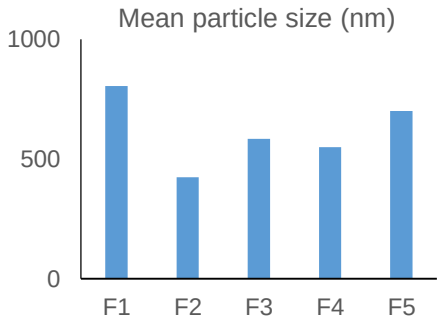


*Fig. 1. Histogram of mean particle sizes for all nano-structured lipid carriers formulations*

*Table 2. Mean particle size, zeta potential, percent entrapment efficiency, and percent drug loading measurements for all formulations*

| Formulation | Mean particle size (nm) | Poly-dispersity index | Zeta-potential | E E% | DL% |
|---|---|---|---|---|---|
| F1 | 805.53±39.5 | 0.361±0.145 | -4.87±1.21 | 75.04 | 7.70 |
| F2 | 423.99±12.73 | 0.296±0.015 | -5.2±1.09 | 27.30 | 2.94 |
| F3 | 584.85±28.67 | 0.349±0.011 | -3.34±1.51 | 57.84 | 6.04 |
| F4 | 549.12±9.8 | 0.287±0.027 | -10.59±2.74 | 58.87 | 6.14 |
| F5 | 700.12±21.23 | 0.291±0.105 | -4.87±1.43 | 64.66 | 6.70 |

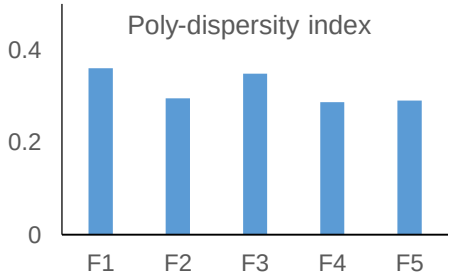


*Fig. 2: Histogram of polydispersity index for all nano-structured lipid carriers' formulations*

The histogram in Fig. 3 depicts the zeta-potential of all NLC formulations. All the NLC particles were found to bear negative charges which is expected for nanoparticles dispersions in water. Generally, the magnitude were low with the highest value was shown with F4 (-10.59 mV). Zeta-potentials of more than 30 mV are required for electrical stabilization of nanoparticles (31). Such systems might be stabilized by addition of low percentage of electrolytes such as sodium acetate.

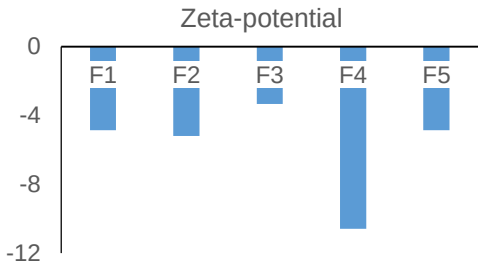


*Fig. 3. Histogram of mean zeta potential for all nano-structured lipid carriers' formulations*

All the prepared formulations showed EE% in the range from 57% to 75% except F2 exhibited a value of only 27%. This give rise to a possible correlation between the increases in surfactant ratio and the lowering of the lipid entrapment capacity as a result of drug leakage from the particles. F1 (containing stearic acid alone) showed the highest EE% which is in agreement with Ibrahim et al. (32). F4 (containing 1: stearic to Dynasan) showed an EE% of 58.87% which is considered a reasonable value. The DL% results were parallel to the EE% ranging from 2.94% to 7.70%. This is considered acceptable with a relatively low-dose drug such as Val.

Particles images for all formulations except F5 obtained by scanning electron microscope are shown in Fig. 4. All the images clearly demonstrated almost a spherical shape for the Val-loaded NLC. The presence of various size species was identified and generally the particle sizes appeared smaller than those determined by light scattering. The use of higher magnification powers was not useful as it resulted in fusion of the particles. This is a common difficulty in processing of SEM images for many lipid based nanoparticles.

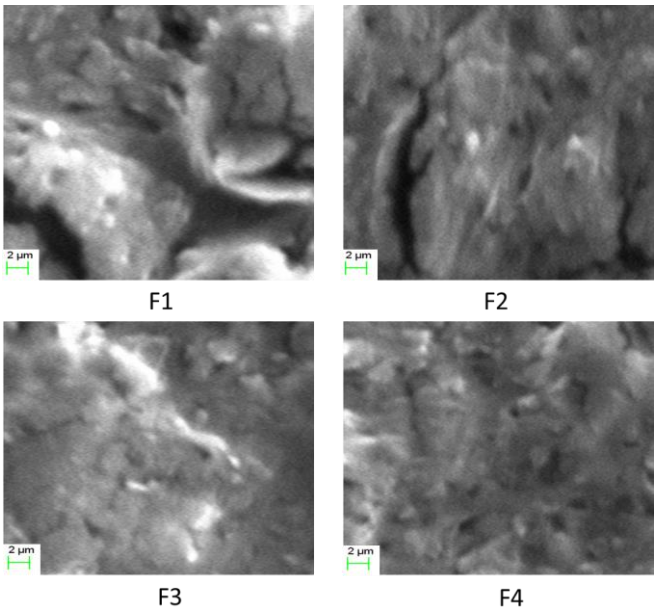


*Fig. 4. Scanning electron micrographs for nanostructured lipid carrier formulations F1, F2, F3, and F4. All images were obtained using 10,000 x magnification power.*

Fig. 5 depicts the DSC thermogram of pure Val, a drug-free F2, F2, F4, and F5. The pure Val showed an endothermic peak at 100.2°C representing the melting of the crystalline form. The blank F2 thermogram showed a sharp endothermic melting peak of stearic acid at 73.6°C. The disappearance of Val melting peak was witnessed in all thermograms of F2, F4, F5 indicating the complete amorphous nature of the loaded Val in the prepared NLC formulations. F2 thermogram showed a slight shift in the stearic acid peak compared with the blank peak. For both F4 and F5,

fusion of the lipid melting peaks was shown to an in-between melting temperature based on the ratios of the lipid components. The presence of the oil did not alter the crystallinity of the lipid specifically for stearic acid. No peak disappearance, broadness or extreme shifting was observed.

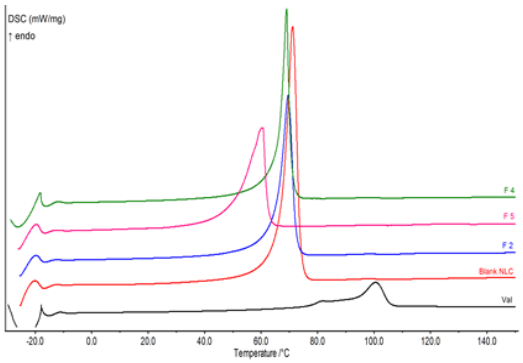


*Fig. 5. Differential scanning calorimetric thermograms for pure valsartan and selected nano-structured lipid carriers' formulations.*

Fig. 6 shows the in vitro release profile of Val from all NLC formulations. It is clear that both F2 and F4 showed a fast release with high initial burst (after 0.5 h) of 63.2% and 51.23%, respectively. Both formulations reached a complete release within 2 h. On the other hand, F3 and F5 exhibited a slow release pattern starting at 24.21% and 15.24%, respectively and a maximum cumulative % release after 24 h of less than 60%. F1 showed an intermediate release profile between the two groups with a typical bi-phasic release of initial fast release period in the first three hours followed by a slow release period from 3 to 24 h. It is obvious that the surfactant ratio affects the rate of drug release and highly correlated. The higher the ratio of the surfactant is the faster is the Val release rate. This can be tailored to various biopharmaceutical applications and delivery needs. This can be envisioned by the possibility of surfactant accumulation on the surface of Val nanoparticles resulting in reducing the interfacial tension with water and enhance particles wettability. The presence of more than one lipid species was found to highly affect the Val release. Dynasan, a glyceryl tristearate ester, presence in F4 accelerated the Val release while Imwitor, a partial glyceryl stearate with 50% monostearate, delayed the Val release. This is in contrast with other reports in the literatures for SLN claiming the slow transformation of long chain fatty acid triglycerides (such as Dynasan) from the less stable α form to stable β form would result in less burst release effect compared with mono and mixed glyceride esters with short chain fatty acids (Imwitor) where drug expulsion from the stable β form rapidly starts (33). It is possibly envisaged the possible esterification of the free carboxylic acid group in the structure of Val with the free hydroxyl mono- and di-glycerides resulting in retention of significant portion of Val within the matrix of F5 NLC.

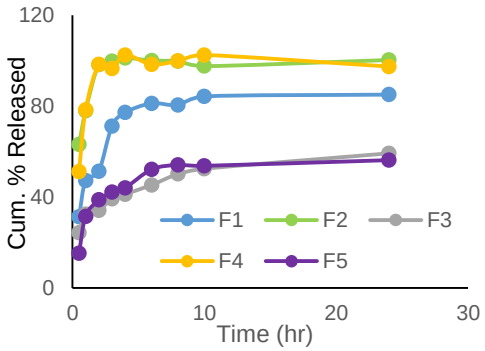


*Fig. 6. Cumulative percent release of valsartan from all nano-structured lipid carriers formulations against time.*

The ultrasonic melt-emulsification method has a number of advantages including simplicity with minimum stressful condition and deprived of toxic organic solvents. However the high polydispersity index of the produced particles is considered a common shortcoming (34). The use of Tween 80 as the main surfactant in the preparation of NLC can be a useful approach to surmount the possible particles aggregation problem resulting from the low magnitude of the zeta-potential values (35).

F4 (containing 1:1 stearic to Dynasan) combines the best attributes among all the prepared NLC formulations with relatively high EE and zeta-potential and relatively low particle size and polydispersity. On top of all this, it has been able to achieve the target of enhancing Val solubility and dissolution.

## 4. Conclusion

The Val-loaded NLC were prepared with a simple reproducible technique. Two of the prepared formulations F2 and F4 successfully enhanced the release of Val and can be considered a visible solution for improving the dissolution-dependent poor gastrointestinal absorption of Val.

**Acknowledgments**

This work was supported by a grant from King Abdullah International Research Center, National Guard Health Affairs, Riyadh, Saudi Arabia (Grant No. SP15/126). The funding agency had no role in study design, data collection and analysis, decision to publish, or preparation of the manuscript.

## References

[1] A. Puri, K. Loomis, B. Smith, J.H. Lee, A. Yavlovich, E. Heldman, et al. Critical reviews in therapeutic drug carrier systems **26**(6), 523 (2009).
[2] A. H. Huang, S. Krishnan, Preparation of injectable doxorubicin/liposome suspension. Google Patents; 1990.
[3] J. B. Bassett, R. U. Anderson, J. R. Tacker, The Journal of urology **135**(3), 612 (1986).
[4] R. Abra, L. S. S. Guo, Amphotericin B/cholesterol sulfate composition and method. Google Patents; 1993.
[5] Y. Hattori, E. Hara, Y. Shingu, D. Minamiguchi, A. Nakamura, S. Arai, et al. Biological & pharmaceutical bulletin. **38**(1), 30 (2015).
[6] G. Vulugundam, K. Kumar, P. Kondaiah, S. Bhattacharya, Organic & biomolecular chemistry **13**(14), 4310 (2015).
[7] S. Beg, S. Swain, H. P. Singh, Ch. N. Patra, M. E. Rao, AAPS PharmSciTech. **13**(4), 1416 (2012).
[8] S. Das, A. Chaudhury, AAPS PharmSciTech. **12**(1), 62 (2011).
[9] M. Jumaa, B. W. Muller, official journal of the European Federation for Pharmaceutical Sciences. **9**(3), 285 (2000).
[10] R. Cavalli, O. Caputo, M. R.Gasco, International Journal of Pharmaceutics. **89**(1), R9 (1993).
[11] S. Mukherjee, S. Ray, R. S. Thakur, Indian journal of pharmaceutical sciences. **71**(4), 349 (2009).
[12] R.Mozafari, Nanocarrier Technologies: Frontiers of Nanotherapy: Springer Netherlands; 2006.
[13] R. H. Muller, K. Mader, S. Gohla, European journal of pharmaceutics and biopharmaceutics : official journal of Arbeitsgemeinschaft fur Pharmazeutische Verfahrenstechnik eV. **50**(1), 161 (2000).
[14] W. Mehnert, K. Mäder, Advanced Drug Delivery Reviews. **47**(2–3), 165 (2001).

[15] D. Hou, C. Xie, K. Huang, C. Zhu, Biomaterials. **24**(10),1781 (2003).
[16] A. zur Muhlen, C. Schwarz, W. Mehnert, European journal of pharmaceutics and biopharmaceutics : official journal of Arbeitsgemeinschaft fur Pharmazeutische Verfahrenstechnik eV. **45**(2), 149 1998.
[17] S. P. Vyas, R. K. Khar, Controlled Drug Delivery - Concepts and Advances: Vallabh Prakashan; 2002.
[18] P. K. Gupta, J. K. Pandit, A. Kumar, P. Swaroop, S. Gupta, T Ph Res. 3, 117 (2010).
[19] H. Li, X. Zhao, Y. Ma, G. Zhai, L. Li, H. Lou, Journal of Controlled Release. **133**(3), 238 (2009).
[20] M. Uner, G. Yener, International journal of nanomedicine. **2**(3), 289 (2007).
[21] M. Radtke, R. H. Muller, Proc Int Symp Control Rel Bioact Mater. **27**, 309 (2000).

[22] R. H. Müller, M. Radtke, S. A.Wissing, International Journal of Pharmaceutics. **242**(1–2), 121 (2002).
[23] M. Uner, Die Pharmazie. **61**(5), 375 (2006).
[24] E. B. Souto, R. H. Muller, Journal of microencapsulation. **22**(5), 501 (2005).
[25] A. Beloqui, M. A. Solinis, A. R. Gascon, A. del Pozo-Rodriguez, A. des Rieux, V. Preat, Journal of controlled release : official journal of the Controlled Release Society. **166**(2), 115 (2013).
[26] A. J. Almeida, E. Souto, Adv Drug Deliv Rev. **59**(6), 478 (2007).
[27] J. Robinson, V. H. L. Lee, Controlled Drug Delivery: Fundamentals and Applications, Second Edition. 2 ed: Taylor & Francis; 1987.
[28] A. E. B. Yassin, A. Albekairy, A. Alkatheri, R. K. Sharma, DIG J NANOMATER BIOS. **8**(2), 905 (2013).
[29] G. Flesch, P. Muller, P. Lloyd, Euro J Clin Pharmacol. **52**(2), 115 (1997).
[30] S. Kashanian, A. H. Azandaryani, K. Derakhshandeh, Int J Nanomedicine. **6**, 2393 (2011).
[31] R. P. Thatipamula, C. R. Palem, R. Gannu, S. Mudragada, M. R. Yamsani, Daru **19**(1), 23 (2011).
[32] W. Ibrahim, A. Al-Omrani, A. E. B. Yassin, Int J of Nanomed. **9**, 129 (2014).
[33] H. Bunjes, K. Westesen, M. H. J. Koch, Int J Pharm. **129**, 159 (1996).
[34] P. M. Bummer, Crit Rev Ther Drug Carrier Syst. **21**, 1 (2004).
[35] F. Liu, J. Yang, L. Huang, D. Liu, Pharm. Res. **13**, 1642 (1996).